Toughening Behavior of Elastomer-Modified Polycarbonates Based on the J-Integral

CHANG-BING LEE *and* FENG-CHIH CHANG*

Department of Applied Chemistry
National Chiao-Tung University
Hsinchu, Taiwan, Republic of China

The J-integral method to determine the fracture toughness of tough and ductile polymeric materials previously developed has been applied to the elastomer-modified polycarbonates. This investigation compares three different methods to obtain Jc: the conventional crack growth length, the stress whitening zone, and the newly developed hysteresis method. Jc values obtained from these three comparative methods are fairly close. The hysteresis method has the advantage over the other two methods of obtaining Jc without requiring the measurement of the crack growth length or the stress whitening zone, therefore avoiding the controversy in defining crack blunting. Results also indicate that the effect of elastomer quantity in polycarbonate on Jc is insignificant as long as the crack is in a stable condition. Higher elastomer contents in polycarbonate result in higher $dJ/d\Delta a$, $dJ/d\Delta l$, and tearing modulus (Tm). This indicates that the elastomer toughening mechanism is due to the increase of the energy required for crack growth extension. The hysteresis loss energy is directly related to the size of the crack tip plastic zone, and the presence of more elastomer indeed increases the crack tip plastic zone, thus making the polycarbonate tougher. Besides, the presence of elastomer tends to increase the crack initiation displacement and shift the failure modes from an unstable fracture. Jc and the criterion for crack initiation based on rate change of hysteresis energy are discussed in detail.

INTRODUCTION

Linear elastic fracture mechanics (LEFM) may strictly be applied to those materials that obey Hooke's law where the stress is proportional to infinitesimal strain. However, the basic LEFM may also be applied to materials that exhibit inelastic deformation around the crack tip, provided that such deformation is confined to the immediate vicinity of the crack tip and the bulk of the body still exhibits linear elastic properties. A means of identifying a unique parameter to characterize the failure of materials that exhibit nonlinear elastic and extensive crack tip plasticity was developed by Rice (1) and applied in polymeric materials by several investigators (2–15). The original derivation of J is strictly valid only for linear or nonlinear elastic materials in which the unloading occurs down the same path as the initial loading (16). Nevertheless, in practice, the use of J or modified J has been successfully applied in many tough and ductile materials (2–15). J may be defined in terms of energy as the rate of decrease of potential energy with crack length. The

criterion for the onset of crack growth is when $J \geq$ Jc. For a perfectly elastic body, J is equivalent to the fracture energy or the strain energy release rate G. Jc is defined as the crack initiation energy, according to ASTM E813-81, and can thus be obtained by the intersection of the crack blunting line and the resistance curve (R-curve). However, the crack blunting phenomenon is highly complicated, and the validity of such an approach is still an open question (11, 13). Besides, the existence of hysteresis, normally observed from most ductile polymeric materials (11, 17, 18) but essentially neglected in J derivations, makes the definition of Jc even more confusing. Thus the Jc obtained from ASTM E813-81 may or may not be the true crack initiation energy. However, it does serve the purpose as an engineering parameter in determining the toughness of materials (13).

Zhang (12) investigated the ABS (acrylonitrile-butadiene-styrene) fracture toughness to obtain Jc by two methods, by the whitening zone (consisting of the real crack growth and crack front damage zone) of the cryogenic fracture surface and by the conventional crack growth zone. The fracture process includes both crack initiation and crack growth.

Crack initiation energy consists of elastic, viscoelastic, and inelastic energies. Jc, the crack initiation energy, obtained from the stress whitening method is consumed in crack blunting and crack tip plasticity. The hysteresis (loss) energy at any stage of the cracking process should correlate to the size of the crack tip plastic zone and therefore the observed crack tip stress whitening zone. The hysteresis contribution from the time-dependent viscoelasticity is considered insignificant or near constant under such slow deformation rate conditions. The crack tip plastic zone can be a combination of shear yielding, crazes, and microvoids from elastomer-matrix debonding, depending on the selections of matrix and elastomer. For the ductile polymeric materials, if the size of the precrack plastic zone exceeds a critical value and the stored potential energy is less than a certain value at the onset of crack initiation, the crack developed later will propagate within the domain of the plastic zone and result in a stable fracture as long as the crack tip front runs within the plastic zone. If the precrack plastic zone is too small for some relatively brittle or notch-sensitive materials (such as PS, SAN, or thick PC) while the stored potential energy exceeds a certain level, the high stress energy release rate due to crack propagation will lead to an unstable and brittle failure. In this study, we intend to describe the relationship between hysteresis energy and the observed stress whitening.

EXPERIMENTAL

Polycarbonate (PC) (MFR = 15) and the elastomer employed were previously described (16). Injection molded PC and the elastomer modified PC specimens with dimensions of $20 \times 90 \times 10$ mm were prepared on an Arburg injection molding machine. A starter crack of one-half depth was initiated by a saw cut and then sharpened with a fresh razor blade. All the notched specimens were annealed near at 120°C for 2 h to release the residual stress prior to standard three-point bend testing. Some specimens with 10% width of the side groove were also prepared in order to compare results from the specimens without the side groove. The J-integral testing method was carried out according to the multiple-specimen method in ASTM E813-81 at ambient conditions and at a testing rate of 2.0 mm/min with a span-to-width ratio of 4. The crack growth length and the related stress whitening zone were measured at the center of the fracture surface by freezing the tested specimens in liquid nitrogen then breaking with a TMI impacter. Tensile yield stress and modulus were measured by using the standard injection molded specimens (1/8 in) with an extensometer (ASTM D638, Type I). The Poisson's ratio of polycarbonate is assumed to be 0.41. Crack growth and the stress whitening zone were measured from the fractured surfaces by means of a traveling microscope. Hysteresis tests were carried out by loading at a predetermined displacement and then re-

turning at the same rate. The J-integral value for a three-point bend specimen with $S/W = 4$ is given in the following equation (8):

$$J = 2 \cdot U/Bb \qquad (1)$$

U is the input energy of the specimen, which is the area under the load vs. displacement curve. B is the specimen thickness, and b is the ligament length. In the conventional crack growth method, the J value at the onset of crack growth, Jc, is determined by the intersection of the resistance curve and the blunting line, which can be calculated as

$$J = 2 \cdot 6_y \cdot \Delta a \qquad (2)$$

where 6_y is the uniaxial yield stress and Δa is the crack growth length when crack blunting. In the stress whitening zone method Jc is determined as the intersection of the crack blunting and the crack growth lines. The major difference between this method and the conventional crack growth method is that the blunting line comes from experimental data while *Eq 2* is employed in the conventional method. The size criterion suggested by ASTM is expressed in terms of J and is

$$B, (W - a) > 25 \left(Jc/6_y \right) \qquad (3)$$

RESULTS AND DISCUSSION

Fracture Surface Morphology

Similar to Zhang's results (12), a stress whitening zone occurs ahead of the initial crack tip when the applied load is above a certain level. This crack tip stress whitening zone continues to exist and grow even after crack initiation. The photograph of the cryogenic fracture surface of a typical elastomer-modified PC (5% elastomer) shows that the boundary line between the crack growth and the crack tip stress whitening zones is well defined and the crack growth front advances evenly across the whole specimen. The crack growth zone (Δa) is located between lines A and B, and the crack tip stress whitening zone ($\Delta l - \Delta a$) is between lines B and C. The stress whitening zone (Δl) defined in this study includes the crack growth length and the crack tip stress whitening zone, which is the zone between lines A and C measured at the center of the specimen. The zone above line C is considered an undamaged or less affected zone. The boundary line between the stress whitening and the undamaged zones is relatively less well defined. The boundary of the crack tip blunting cannot be identified from this fracture surface morphology. *Figure 1b* shows the detailed SEM microscopic features of the crack growth zone (between lines A and B on *Fig. 1a*) where the surface is very rough with extensive elastomer-initiated yielding. *Figure 1c* shows the cryogenic impact fracture surface of the crack tip stress whitening zone (between lines B and C on *Fig. 1a*), which is characteristic of brittle fracture with negligible localized shear yielding and many empty holes
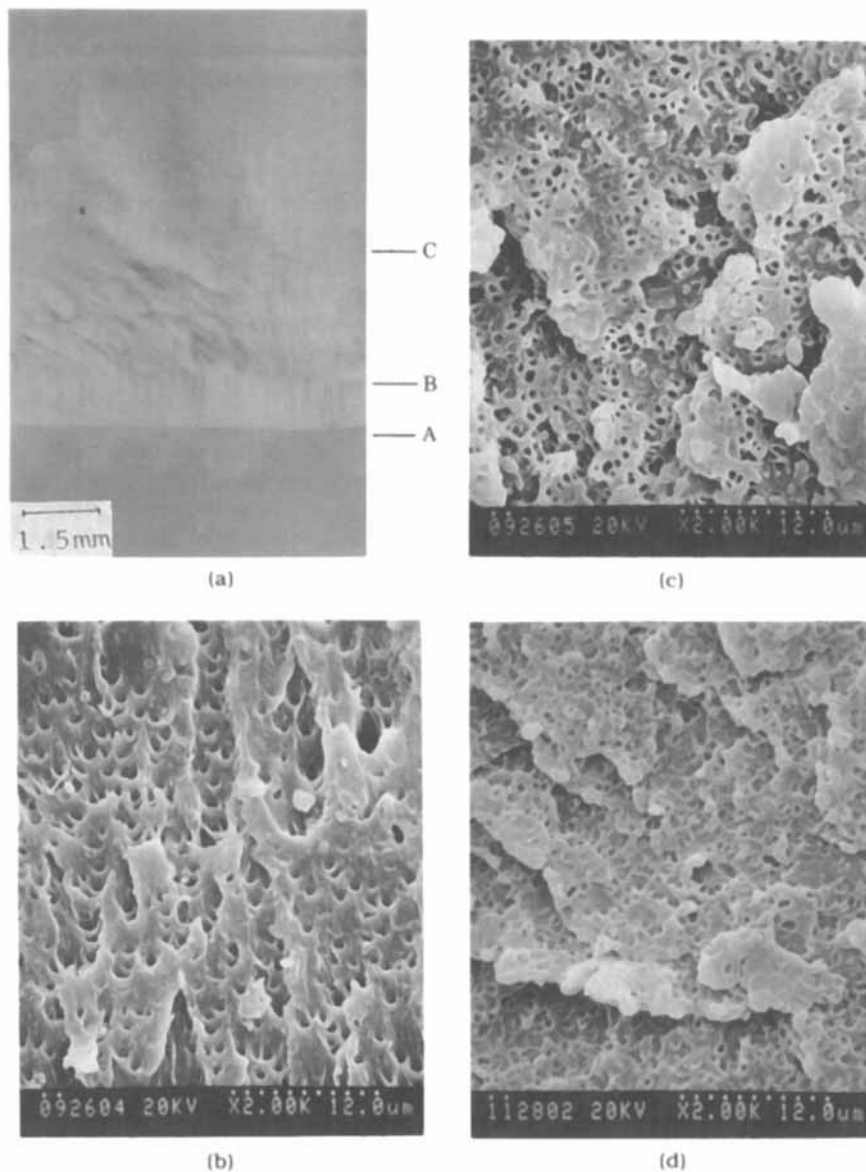
Fig. 1. Fracture surface of PC + 5% elastomer. a) crack growth zone (between lines A and B) and crack tip stress whitening zone (between lines B an C); b) surface micrograph in the crack growth zone; c) surface micrograph in the crack tip stress whitening zone; d) surface micrograph in the undamaged zone.

due to rubber cavitation. This means the rubber particles are triaxially stretched and then collapsed, thus creating numerous voids at the rubber/matrix interface prior to cryogenic fracture. The bonding between rubber and matrix is expected to be severely weakened, and the subsequent cryogenic fracture is able to pull out the rubber particles from the PC matrix, leaving many empty rubber sites. The undamaged zone (*Fig. 1d*, above line C in *Fig. 1a*) is very similar to the crack tip stress whitening zone (*Fig. 1c*) except that less elastomer-initiated localized yielding and fewer rubber cavitations are present. This result indicates that most of the rubber particles are unaffected and still well-bonded to the PC matrix in this undamaged zone prior to the cryogenic fracture. Therefore, the formation of the crack

tip stress whitening zone is due to the void formation by the rubber-matrix debonding to relieve the plane strain tensile hydrostatic stress during the deformation process. Of course, the crazes may also be partially responsible for the observed stress whitening zone but this cannot be verified by the fracture surface morphology.

Figure 2 shows additional fracture surfaces, virgin PC and PC + 2.5% elastomer, for comparing the results of the stable and the unstable fractures. *Figure 2b* illustrates the unstable fracture surface of the virgin PC with torn plate-like plastic shear bands. *Figure 2d* shows the stable crack growth region of PC + 2.5% elastomer; it is very similar to *Fig. 1b* except that the extent of the elastomer-initiated yielding is less.
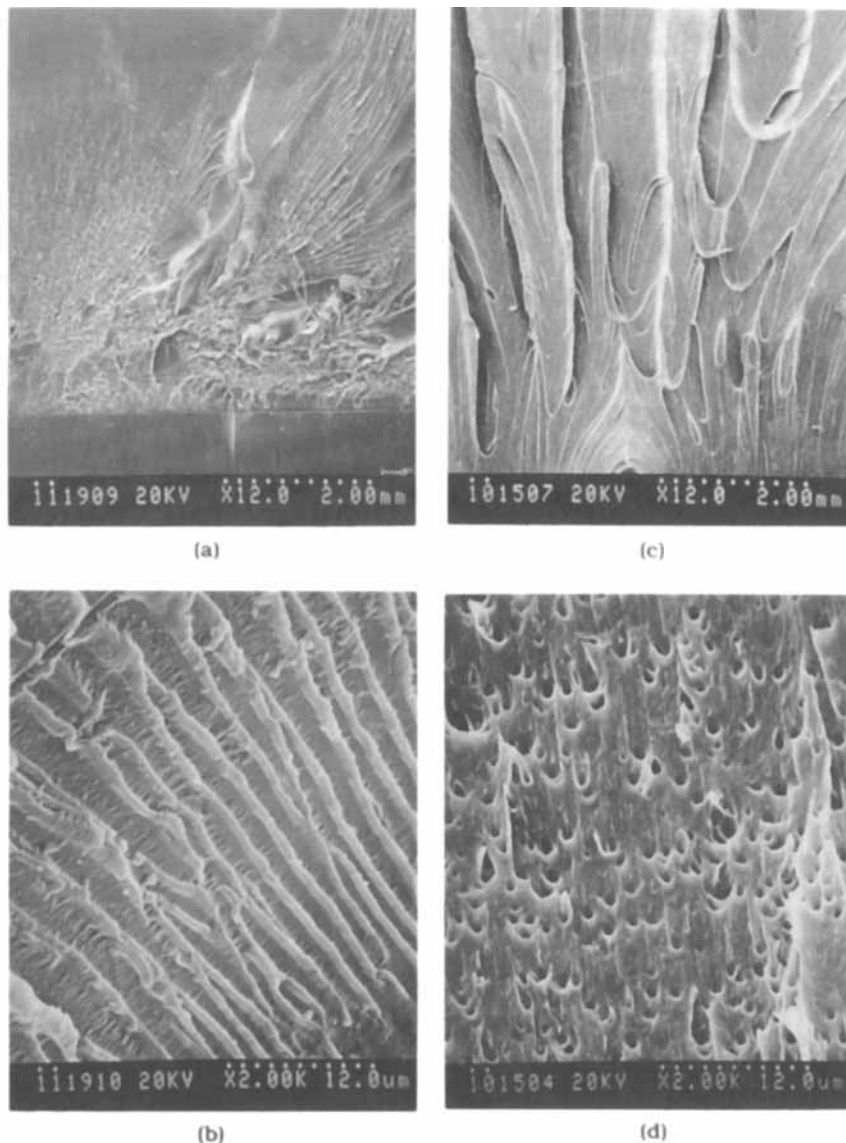
Fig. 2. Fracture surfaces of virgin PC and PC + 2.5% elastomer. a) virgin PC, unstable fracture; b) teared shear bands of the unstable fracture virgin PC; c) PC + 2.5% elastomer, stable fracture; d) PC + 2.5% elastomer, crack growth zone with extensive elastomer-initiated localized shear yielding.

Figure 3 shows the plot of the stress whitening zone length (Δl, measured at the center of the specimen) vs. the crack growth length (Δa) from a typical elastomer-modified PC (PC + 10% elastomer). The slope is higher at the early stages of deformation but later becomes lower, as shown in *Fig. 3*. The intersection between these two lines is believed to be related to the crack initiation. *Figure 4* expresses the relation between the crack tip stress whitening distance ($\Delta l - \Delta a$) and the crack growth length (Δa) showing a similar trend as in *Fig. 3*.

Crack Blunting and Stress Whitening

As mentioned previously, the existence of crack blunting is still an open question, and it cannot be identified from the fracture surface in this study. Therefore, the assumed critical crack growth length
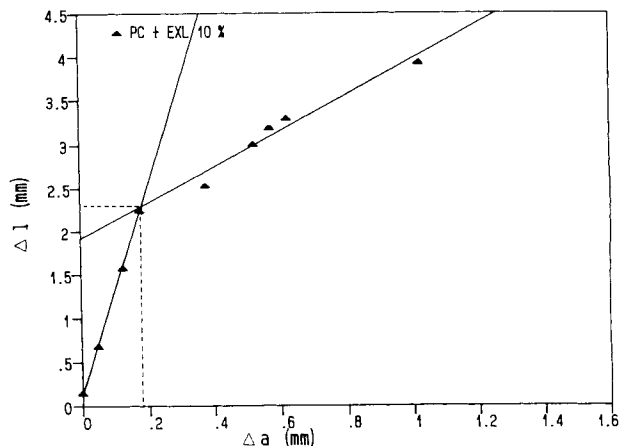

Fig. 3. Plot of the stress whitening zone length (Δl) vs. crack growth length (Δa) for PC + 10% elastomer.
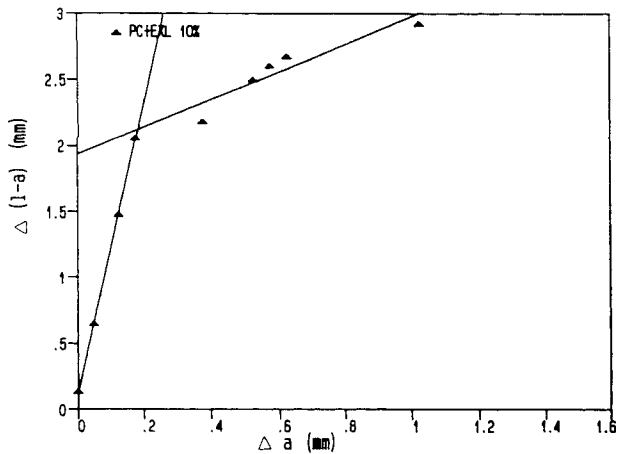
Fig. 4. Plot of the crack tip stress whitening $(\Delta l - \Delta a)$ vs. crack growth length for PC + 10% elastomer.

Fig. 5. Load displacement curve for PC + 2.5% elastomer.

$(\Delta a$ at the crack initiation) has to be obtained from the disputable *Eq 2. Figure 5* is a typical load-displacement curve for an elastomer-modified PC (2.5% elastomer), in which the specimens were deformed and released at points A through E. These specimens were purposely selected for further investigation of their stress whitening zone from a side view. *Figure 6* illustrates the side view micrograph at an early stage of deformation (*Fig. 5*, point A), where the phenomenon of crack tip blunting can be easily observed. The optical micrographs of side views at early crack blunting (point A), before crack initiation (point B), near crack initiation (point C), after crack initiation (point D), and late crack growth (point E) are illustrated in *Figs. 7a* through *7e*. Since all these photographs were taken from the surfaces of the original thick specimens, the observed stress whitening zones are representative only of plane-stress stress whitening. The observed stress whitening zone is relatively less defined at lower loading (*Fig. 7a*), and the zone domain gradually becomes well defined at later stages of deformation (*Figs. 7b* to *7e*). The stress whitening zone at the center of the specimen is expected to be longer but narrower than at the surface as demonstrated in *Fig. 8. Figures 8b* through *8e* are the side-view photographs of the specimens deformed to near crack initiation (point C, *Fig. 5*) and then polished to various thicknesses according to *Fig. 8a*.

J Data From Crack Growth Length

Typical plots of *J*-integral values against crack growth lengths, with and without the side groove, are illustrated in *Figs. 9* and *10. Jc* values were then determined from these resistance curves according to the ASTM E813-81; the results are summarized in *Table 1. Jc* values thus obtained are almost independent of elastomer content. Because of the unstable fracture nature of the virgin PC, the *Jc* was calculated from the corresponding *Kc* (ASTM 1399). The presence of the side groove slightly re-
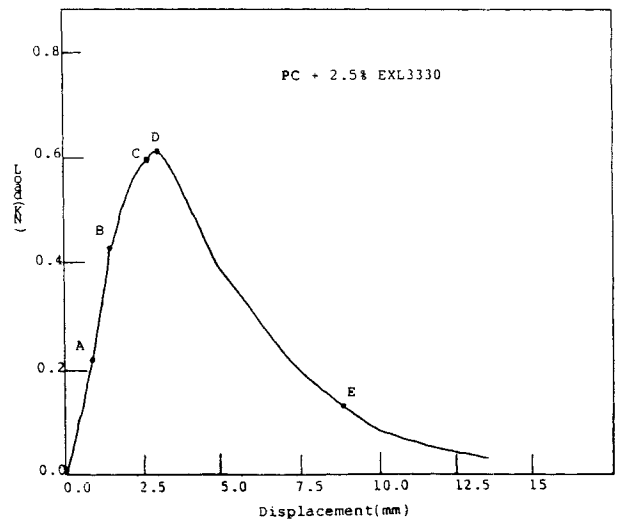

Fig. 6. Crack tip blunting for PC + 2.5% elastomer at point A in Fig. 5.

duces the *Jc* values but maintains about the same values of $dJ/d\Delta a$ from all the elastomer-modified polycarbonates. $dJ/d\Delta a$ can be considered the resistance of a material to stable crack extension. Paris (19) developed the tearing modulus concept to describe the stability of ductile crack growth. Ductile tearing instability in some engineering thermoplastic blends has been previously reported (20). This concept postulates that instability occurs if the elastic shortening of the system exceeds the corresponding plastic lengthening required for crack extension. In this theory, a nondimensional parameter tearing modulus, *Tm*, can be expressed as

$$Tm = \frac{E}{6_y^2} \frac{dJ}{d\Delta a} \qquad (4)$$

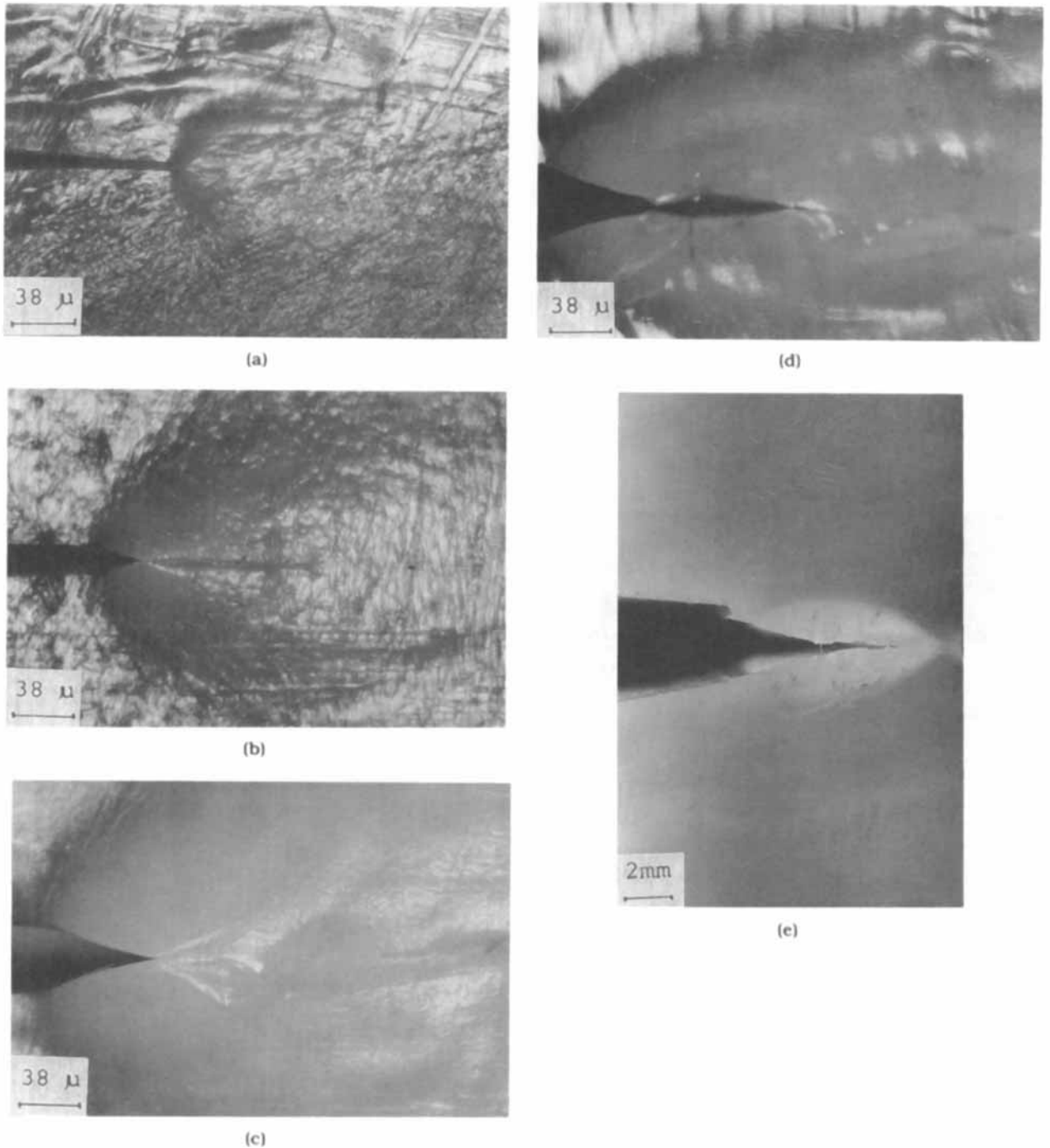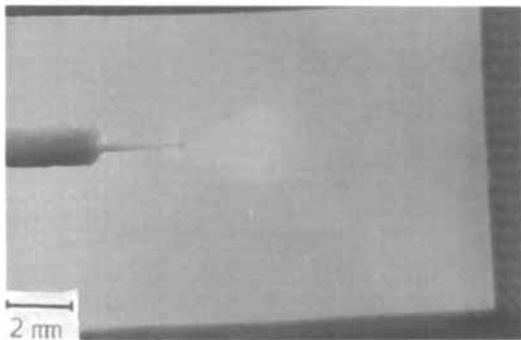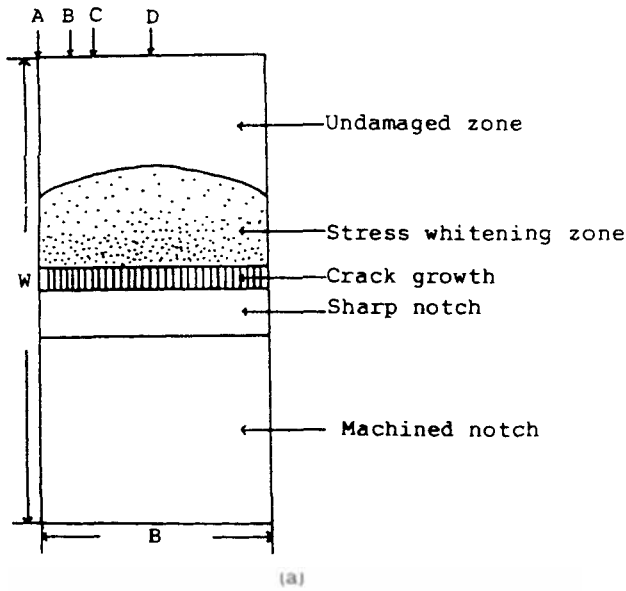where *E* is the Young's modulus, 6_y is the yield

Fig. 7. *Side-view photographs for PC + 2.5% elastomer at various stages of deformation: a) early crack blunting, point A in Fig. 5; b) before crack initiation, point B in Fig. 5; c) near crack initiation, point C in Fig. 5; d) after crack initiation, point D in Fig. 5; e) late crack growth, point E in Fig. 5.*

stress, J is the J-integral, and Δa is the crack growth length. *Figure 11* shows the plots of $dJ/d\Delta a$ and Tm vs. the elastomer contents. Both $dJ/d\Delta a$ and Tm increase with increasing elastomer content. This result indicates that the presence of more elastomer increases the capability to withstand crack extension and thus toughens the PC matrix. Specimen size for both Jc and Kc determinations em-
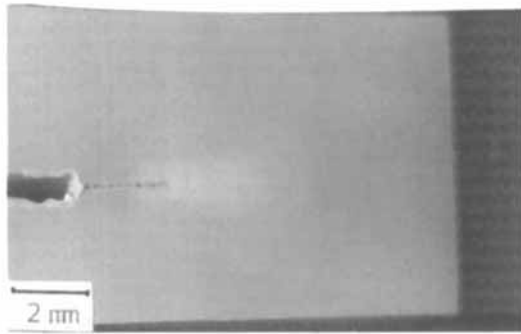
ployed in this study are within the plane-strain conditions suggested by ASTM standards as *Eq 3*.
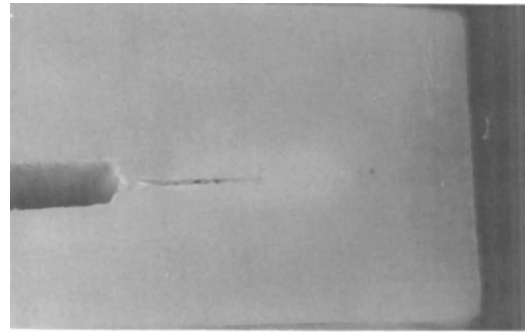
J Data from the Crack Stress Whitening Zone

The typical plots of J vs. stress whitening zone (Δl) are shown in *Figs. 12* and *13*; the rest of the information is summarized in *Table 2*. In the conventional crack growth method, the slopes of the
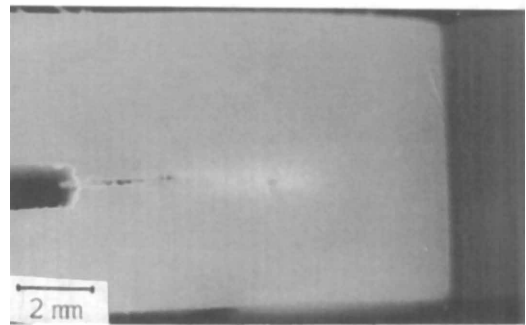
Fig. 8. Side-view photographs from center to surface for PC + 2.5% elastomer at point C in Fig. 5: a) fracture drawing showing various zones and locations of polishing the specimen; b) side view from surface, point A in Fig. 8a; c) side view from plane at point B in Fig. 8a; d) side view from plane at point C in Fig. 8a; e) side view from center plane at point D in Fig. 8a.

crack blunting lines are significantly higher than the corresponding *R*-curves, as shown in *Figs. 9* and *10*. This order is reversed in this stress whitening zone method, as illustrated in *Figs. 12* and *13*, where the crack blunting lines are constructed from the experimental data points. *Jc* values obtained from this alternative method (*Table 2*) are fairly

consistent with the previous method based on crack growth length (compare *Tables 1* and *2*).

Figure 14 shows the plots of *Jc* and $dJ/d\Delta l$ (during crack blunting and during crack growth) vs. elastomer content. It is interesting to note that the obtained $dJ/d\Delta l$ decreases during crack blunting but increases during crack growth with the increase

of elastomer content. This means that PC with higher elastomer content requires less energy to create the same size stress whitening zone during crack blunting but requires more energy during crack propagation. This result can be further explained by *Fig. 15*, in which the crack initiation displacement and the corresponding hysteresis energy are plotted against elastomer content. Typically, the stress whitening zone extends gradually and almost linearly with load at early stages of deformation up to the onset of crack growth initiation. *J* may be expressed in terms of elastic and plastic components, as in the following equations.

$$J = J_e + J_p \tag{5}$$

$$J = \eta_e U_e / Bb + \eta_p U_p / Bb \tag{6}$$

$$dJ/d(l) = \eta_e d(U_e)/Bbd(\Delta l) + \eta_p d(U_p)/Bbd(\Delta l) \tag{7}$$

where U_e and U_p are the elastic and plastic components of the total energy, U, respectively, η_e and η_p are their corresponding elastic and plastic work factors, and b is the uncracked ligament $(W - a)$.

Under a displacement controlled test, several major events will occur simultaneously after the onset of crack initiation. First, the crack tip becomes sharper, owing to the freshly formed crack tip. Second, the input energy rate shifts from the original crack blunting into the crack propagation minus the storage stress energy released due to the crack extension. Each event undoubtedly influences both the elastic and plastic components of *J* as indicated in *Eq 7*. These complicated but competitive events, and probably some other reasons not mentioned here, result in the increase of the slope after the onset of crack initiation shown in *Figs. 12* and *13*. The criterion to determine the crack initiation of this stress whitening zone comes from the experimental data points; therefore, *Jc* obtained from this alternative method has more physical meaning than the conventional crack growth method. However,
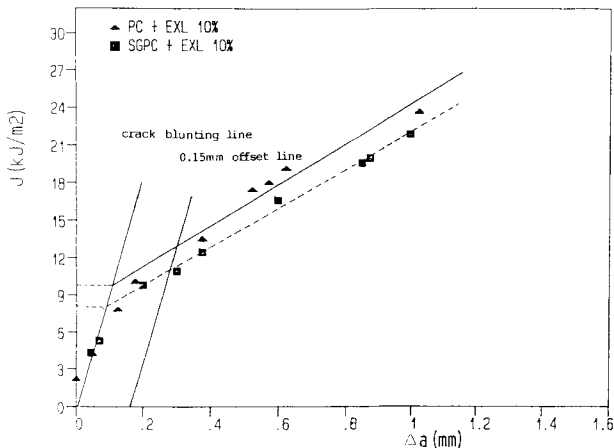

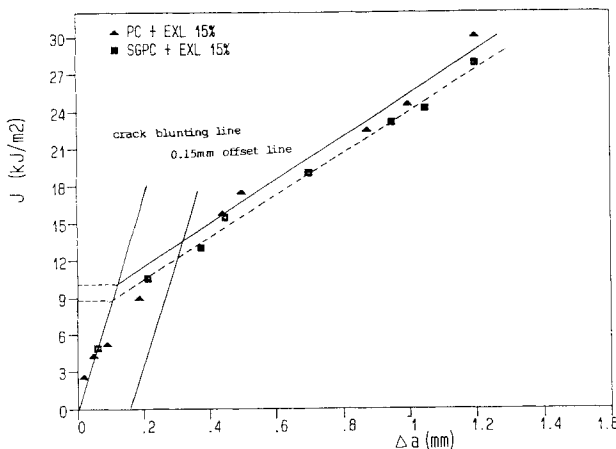Fig. 9. *Plot of J vs. crack growth length with and without side groove for PC + 10% elastomer.*

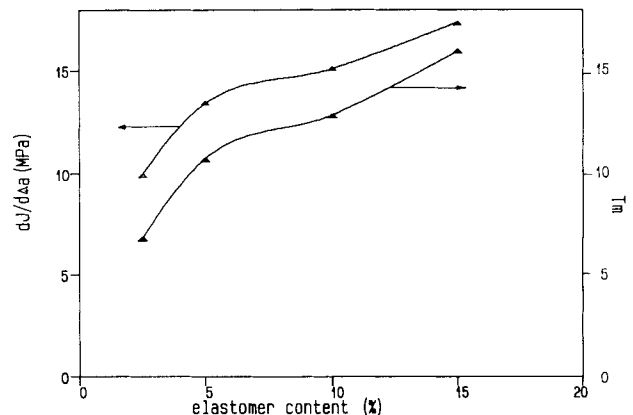Fig. 10. *Plot of J vs. crack growth length with and without side groove for PC + 15% elastomer.*

Fig. 11. *Effect of elastomer contents on dJ/d a and Tm.*

Table 1. Fracture Toughness Data by the Crack Growth Method.

	PC + EXL 0%	PC + EXL 2.5%	PC + EXL 5%	PC + EXL 10%	PC + EXL 15%
E, Mpa	2250	2140	1970	1759	1580
6*y*, Mpa	60.2	56.1	49.6	45.5	41.5
Jc, Kj/m^2	5.4	10.6	10.1	9.9	10.3
Jc, with SG	4.1	8.0	8.4	8.0	8.8
dJ/dΔ*a*, Mpa	—	10.0	13.4	15.1	17.4
dJ/dΔ*a*, (SG)	—	10.2	13.2	14.9	17.1
Tm[a]	—	6.8	10.7	12.8	16.0

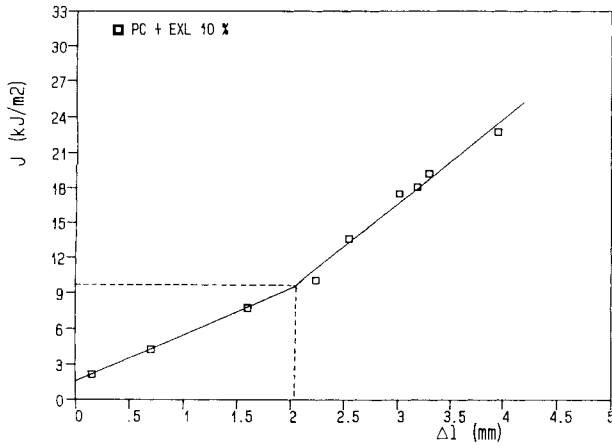[a] $Tm = E/6_y^2 \, dJ/d\Delta a$, from the specimens without side grooves.

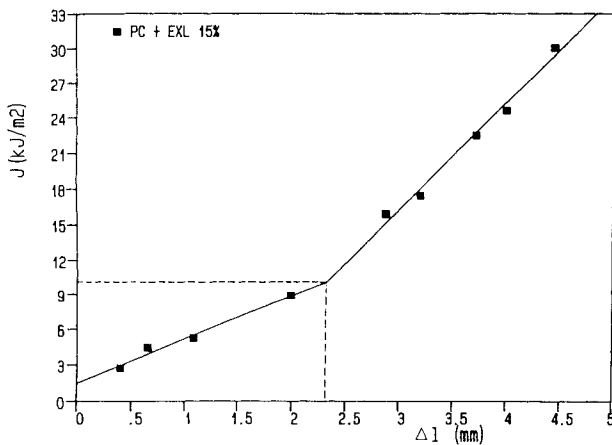Fig. 12. Plot of J vs. stress whitening zone for PC + 10% elastomer.

Fig. 13. Plot of J vs. stress whitening zone for PC + 15% elastomer.

Hysteresis

Hysteresis is defined as the energy dissipated in the strain cycle where the unloading path is below the loading path. Strictly speaking, hysteresis can be applied only when the deformed material returns to its original shape (i.e., zero strain). Here we define the hysteresis or the loss energy as the energy difference between the input and the recovery in a cyclic loading and unloading process, including crack blunting and crack growth. The close relation between the pre-crack hysteresis and the corresponding ductile-brittle transition behavior of polycarbonates and polyacetals has been previously reported [17, 18]. Greater pre-crack hysteresis energy results in a greater crack tip plastic zone and tends to fracture in a ductile mode. *Figure 16* shows the curves of the total load displacement and the load-unload at crack initiation of polycarbonates with various elastomer contents. The results are summarized in *Table 2*. Except for the virgin PC, all the elastomer-modified PCs fracture in a stable manner. The onset of crack initiation occurs just prior to the load maximum, with significant crack propagation occurring near the load maximum, which is very similar to Narisawa's report [21]. The presence of more elastomer results in the expected lower load maximum but higher crack initiation displacement

some systems may not produce the clear stress whitening zone for this method to be applicable, and the conventional crack growth method still must be employed. One drawback of this method arises when the slope difference may not be significant enough to locate accurately the onset of crack initiation. In this study, we found that the slope difference decreases with decreasing elastomer content. Therefore, we suspect that this method may fail in some other ductile polymeric systems. During the crack growth, the slopes of the R-curves, $dJ/d\Delta a$, and $dJ/d\Delta l$ all increase with increasing elastomer content. Therefore, the mechanism of elastomer toughening PC is due to the increase of its capability to resist crack growth extension if the crack is stable. The extents of the observed surface shear yielding in the crack growth zone, which increase with elastomer content, provide additional evidence of the elastomer-toughening mechanism. Virgin PC cracks in an unstable manner, and the fracture surface is composed of mainly torn plate-like shear bands, as shown in *Fig. 2b*. The presence of elastomer tends to shift the crack mode from unstable to stable.
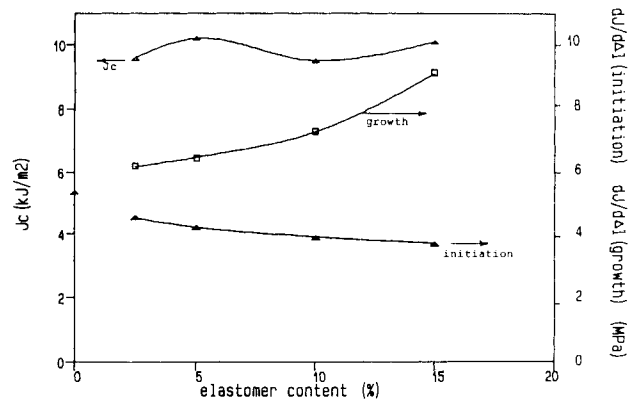

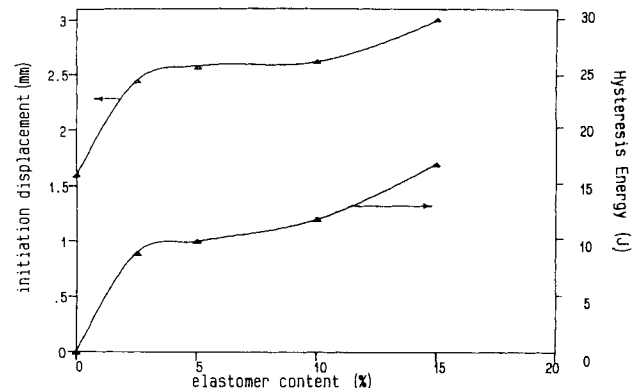Fig. 14. Effect of elastomer contents on Jc and dJ/d Δl.

Fig. 15. Effect of elastomer contents on initiation displacement and hysteresis energy.

Table 2. Hysteresis and Fracture Toughness Data From the Stress Whitening Zone Method.

	PC + EXL 0%	PC + EXL 2.5%	PC + EXL 5.0%	PC + EXL 10%	PC + EXL 15%
Initiation disp, mm	1.60	2.45	2.58	2.62	3.00
Hysteresis[a] ratio	0	0.18	0.21	0.24	0.34
Hysteresis[a] energy, j	0	0.09	0.10	0.12	0.17
Permanent[a] disp, mm	0	0.08	0.14	0.21	0.47
Jc, Kj/m^2	5.4	9.6	10.2	9.5	10.1
$dJ/d\Delta l$, MPa initiation	—	4.5	4.2	3.9	3.7
$dJ/d\Delta l$, MPA propagation	—	6.2	6.5	7.3	9.1

[a] At the crack initiation.

and hysteresis energy (22), as illustrated in *Fig. 16*. Hysteresis energies vs. deformation displacements for PC + 15% elastomer at various stages of loading are shown in *Fig. 17*. The increment of hysteresis energy begins to take off rapidly at 2.74 mm displacement (the intersection of these two lines). We temporarily assume this point is the displacement of the crack initiation. In order to obtain the Jc based

on this hysteresis method, a relation curve between J and displacement must be constructed, as shown in *Fig. 18*. As soon as the critical displacement is determined (from *Fig. 17*), Jc can be obtained from *Fig. 18*. For the purpose of conforming our assumption, a plot of the crack growth lengths (Δa) vs. the corresponding displacements of the same system is shown in *Fig. 19*, where an intersection displacement almost identical (2.72 mm) to that in *Fig. 17* is obtained. This close result is not a coincidence; it is due to the crack initiation. A simple energy balance approach can be used to interpret the cause of the sudden increase of hysteresis energy after crack initiation. The input energy at any stage of deformation can be considered as the combination of the recoverable elastic storage energy and the unrecoverable hysteresis energy.

$$U_i = U_r + U_h \qquad (8)$$

where U_i is the input energy, U_r is the recoverable, elastic storage energy, and U_h is the unrecoverable hysteresis energy. The hysteresis energy consists of energies consumed in plasticity, crazes, microvoids, viscoelasticity (negligible at such a slow rate), and the surface free energy (negligible before crack initi-
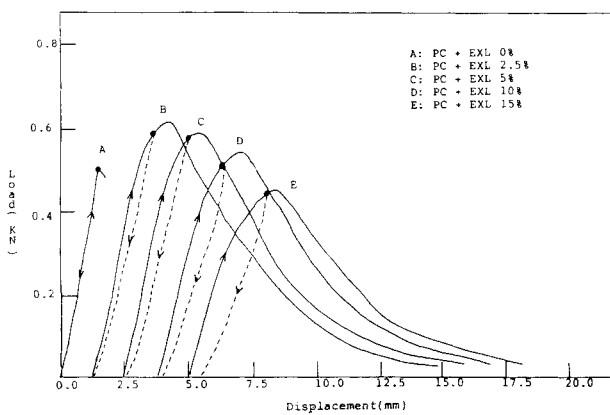

Fig. 16. Load displacement and loading-unloading curves for virgin PC and elastomer-modified PCs.
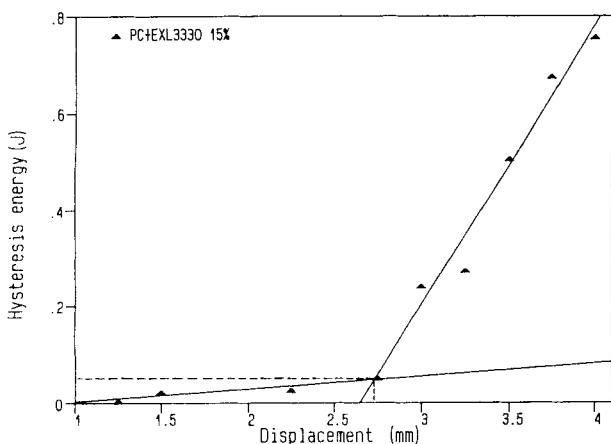

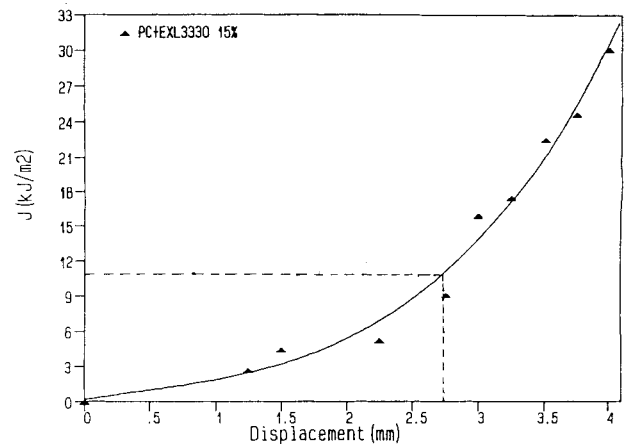*Fig. 17. Plot of hysteresis energy vs. displacment for PC + 15% elastomer.*

Fig. 18. Plot of J vs. displacement for PC + 15% elastomer.

ation). Both the recoverable and the hysteresis energies increase gradually at different rates before crack initiation. After crack initiation, the change of the hysteresis energy, except that from the surface free energy, is relatively insignificant. The energy consumed in creating the new surfaces will shift part of the elastic storage energy into the hysteresis energy and result in a drastic increase of the hysteresis energy immediately after crack initiation. The crack growth length (Δa) at the line intersection from *Fig. 19* is 0.167 mm, which should be considered the critical crack growth length at the onset of crack initiation. The crack growth length of 0.122 mm obtained from *Fig. 10* is considered an artificial length because the blunting line is based on the ideal crack tip blunting given by *Eq 2*. The reliability of that equation in locating crack initiation is still an open question. However, we feel that the crack growth length at the crack initiation derived indirectly from the hysteresis energy is of more physical meaning. *Table 3* summarizes all the data for this particular blend (PC + 15% elastomer) that has been used for these three methods to determine *Jc*. *Table 4* lists the comparative *Jc* values obtained by these three independent methods based on the same set of experimental data.

Whether this hysteresis energy approach is applicable to other ductile polymeric systems requires additional study. Our recent study on HIPS (high impact polystyrene) and ABS (23, 24), which compared the hysteresis method and the conventional crack growth methods (ASTM E813-81 and E813-87), resulted in conclusions similar to those of this report. If the hysteresis approach is proved to be generally feasible, actual measurement of the tedious crack growth length to determine *Jc* will be unnecessary. It requires only construction of a *J* vs. displacement curve and measurement of the corresponding hysteresis energy (preferably from identical multiple specimens) at various stages of deformation. The displacement of crack initiation is located at the intersection of the two straight lines of the plot of hysteresis energy vs. displacement. *Jc* is then obtained from the *J* vs. displacement curve if the displacement at crack initiation is known. Therefore, the controversy over how to define the crack blunting line (9, 11, 13) can be avoided. We feel that this proposed hysteresis approach in the *J*-integral method can also be applied to other materials, such as metals or some composites. If the conventional crack growth method still must be carried out to determine *Jc*, employing this proposed hysteresis energy method means that no extra experimental work is needed to double-check the result.
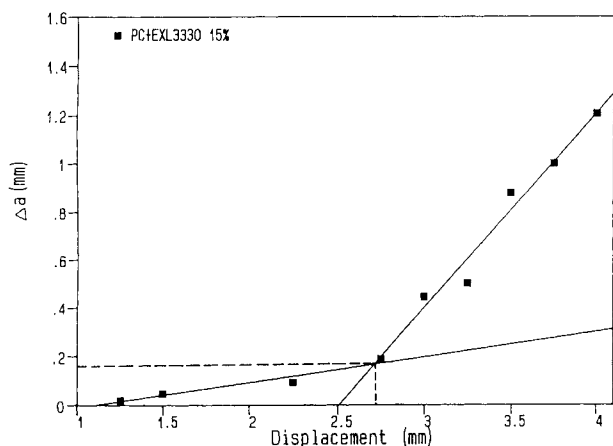
CONCLUSIONS

Jc of the elastomer modified PC determined by the three separate methods, crack growth, stress whitening, and hysteresis energy, are in close agree-

Fig. 19. Plot of crack growth length vs. displacement for PC + 15% elastomer.

Table 4. Comparative Jc and Δ a From Three Methods.

Method	Δa, mm	Jc, Kj/m^2	Jc^d, Kj/m^2
Crack growth (ASTM E813-81)	0.122[a]	10.3	10.3
Stress whitening	0.250[b]	10.1	12.1
Hysteresis	0.167[c]	10.8[e]	10.7

[a] From *Fig. 10*.
[b] Δl first obtained from *Fig. 13*; Δa is obtained from the relation plot between Δl vs. Δa, similar to *Fig. 3*.
[c] From *Fig. 19*.
[d] Use Δa from first column and *Fig. 10* to determine *Jc*.
[e] Use the critical displacement from *Fig. 17* and *Fig. 19* to determine *Jc*.

Table 3. Summarized J Data for PC + 15% EXL3330.

D^a mm	U^b joule	J^c Kj/m^2	Hyster, Ratio	Hyster. E, joule	Δa mm	Δl mm	$\Delta(1-a)$ mm
1.25	0.13	2.66	0.052	0.007	0.02	0.40	0.38
1.50	0.22	4.40	0.098	0.022	0.05	0.66	0.61
2.25	0.27	5.29	0.114	0.030	0.09	1.09	1.00
2.75	0.45	9.07	0.116	0.052	0.19	2.00	1.81
3.00	0.79	15.9	0.300	0.240	0.44	2.88	2.44
3.25	0.88	17.5	0.314	0.274	0.50	3.20	2.70
3.50	1.13	22.5	0.450	0.510	0.87	3.72	2.85
3.75	1.24	24.7	0.500	0.680	1.00	4.00	3.00
4.00	1.51	30.1	0.546	0.760	1.20	4.45	3.25

[a] D: deformation displacement.
[b] U: energy under load-displacement curve.
[c] J: J-integral value, $J = 2 \cdot U/B \cdot b$.

ment. This new hysteresis method does not require the time-consuming crack growth length measurement because locating the critical crack growth length in Jc determination is unnecessary. The increase of elastomer in PC does not significantly change its Jc but results in higher $dJ/d\Delta a$ and tearing modulus. Such results indicate that the presence of elastomer increases the capability of polycarbonate to resist crack extension. The close relation between the elastomer content and the corresponding hysteresis energy provides additional evidence of elastomer toughening of the system.

ACKNOWLEDGMENT

REFERENCES

1. J. R. Rice, *J. Appl. Mech.*, **35**, 379 (1968).
2. C. E. Turner, in *Post-Yield Fracture Mechanism*, p. 23, D. G. H. Latzko, ed., Applied Science Publishers Ltd., London (1979).
3. J. A. Begley and J. D. Landes, in *Fractures Toughness*, ASTM STP 514, p. 1, American Society for Testing and Materials, Philadelphia (1972).
4. E. Plati and J. G. Williams, *Polym. Eng. Sci.*, **15**, 470 (1975).
5. J. M. Hodgkinson and J. G. Williams, *J. Mater. Sci.*, **16**, 50 (1981).
6. M. K. V. Chan and J. G. Williams, *Inter. J. Fracture*, **22**, 145 (1983).
7. S. Hashemi and J. G. Williams, *Polym. Eng. Sci.*, **26**, 760 (1986).
8. S. Hashemi and J. G. Williams, *Polymer*, **27**, 384 (1986).
9. I. Narisawa, *Polym. Eng. Sci.* **27**, 41 (1987).
10. D. D. Huang and J. G. Williams, *J. Mater. Sci.*, **22**, 2503 (1987).
11. I. Narisawa and M. T. Takemori, *Polym. Eng. Sci.*, **29**, 671 (1989).
12. M. J. Zhang, F. X. Zhi, and X. R. Su, *Polym. Eng. Sci.*, **29**, 1142 (1989).
13. D. D. Huang and J. G. Williams, *Polym. Eng. Sci.*, **30**, 1341 (1990).
14. C. B. Lee and F. C. Chang, *Proc. 13th ROC Polym. Symp.*, p. 780, Hsinchu, Taiwan (1990).
15. E. J. Moskala and M. R. Tant, *Polym. Mater.: Sci. Eng.*, **63**, 522 (1990).
16. A. J. Kinloch and R. J. Young, in *Fracture Behavior of Polymers*, p. 82, Elsevier Applied Science Publishers, England (1985).
17. F. C. Chang and H. C. Hsu, *J. Appl. Polym. Sci.*, **43**, 1025 (1991).
18. F. C. Chang and M. Y. Yang, *Polym. Eng. Sci.*, **30**, 543 (1990).
19. P. C. Paris, H. Tada, A. Zahoor, and H. Ernst, in *Elastic-Plastic Fracture: First Symposium*, ASTM STD 668, 5 (1979).
20. M. E. J. Dekkers and S. Y. Hobbs, *Polym. Eng. Sci.*, **27**, 1164 (1987).
21. I. Narisawa and M. T. Takemori, *Polym. Eng. Sci.*, **28**, 1462 (1988).
22. F. C. Chang and L. H. Chu, *Polym. Mater.: Sci. Eng.*, **60**, p. 851 (1989).
23. C. B. Lee, M. L. Lu, and F. C. Chang, *J. Appl. Polym. Sci.*, in press.
24. M. L. Lu, C. B. Lee, and F. C. Chang, *Proc. 14th ROC Polym. Symp.*, p. 875, Hsinchu, Taiwan (1991).